Assessing sampling strategies and soil sensors performance in the detection of field scale variability of plant-available nitrogen

E. Wallor[1], M. Bourouah[2], K.C. Kersebaum[1], R. Gebbers[3]

[1]*Leibniz Centre for Agricultural Landscape Research (ZALF), Institute of Landscape System Analysis, Muencheberg, Germany*
[2]*Hahn-Schickard-Society for Applied Research, Villingen-Schwenningen, Germany*
[3]*Leibniz Institute for Agricultural Engineering and Bioeconomy, Department of Engineering for Crop Production, Potsdam, Germany*

evelyn.wallor@zalf.de

Abstract

Agriculture contributes the strongest to the nitrogen (N) enrichment of ecosystems. It is therefore important to know the spatial distribution of factors influencing N losses or to know the distribution of soil nitrate (NO_3^-) itself. One resource-extensive method to capture NO_3^- variability is the use of sensors. The present study examines the within-field variability of soil mineral N resulting from three sampling strategies and compares outputs of an ion-selective electrode (ISE) and a colorimeter to the results of the N_{min}-method. With regard to sampling, the differences in the measured soil states are more pronounced when grouped by soil texture classes. The sensory measured NO_3^- concentration normally exceeds that of the N_{min}-method. Furthermore, type and quality of the relation between sensory and conventional NO_3^- results depend on the preparation of soil samples and their organic carbon content.

Keywords: soil mineral nitrogen, soil variability, ion selective electrode, colorimeter

Introduction

The variability of plant-available or soil mineral nitrogen (N) at field scale is mainly influenced by the soil texture and its vertical distribution in the soil profile. This is due to the impact of soil texture on soil moisture dynamics which affects denitrification (Giles et al., 2012). Both terms, plant-available and mineral N, consider nitrate (NO_3^-) and ammonium (NH_4^+), with NO_3^- accounting for much more of the soil. Risks to the environment, such as NO_3^- leaching, are caused inter alia by nutrient management that is not adapted to the specific soil inventory and the corresponding hydraulic properties of the field (Galloway et al., 2003). In order to capture the temporal and spatial variability of plant-available N and to ensure site-adapted fertilization, at least two measurements per growing season in a corresponding sampling design are necessary (Nanni et al., 2011). With conventional sampling and soil monitoring at a high spatio-temporal resolution is not economical. Until now, the lack of affordable methods for mapping relevant soil nutrients is a fundamental problem in precision agriculture (Gebbers et al., 2016). To advance research in this area, the present study i) compares the results of three different sampling strategies with respect to the variability of soil mineral N, ii) examines the importance of soil texture on the distribution of soil states,

and ii) investigates the traceability of plant-available NO_3^- in soils by two sensor systems in parallel.

Materials and Methods

Study sites and data

The data used for evaluating sampling strategies for assessing the variability of soil mineral N at field scale were collected on a 20-hectare agricultural site near Beckum, Germany (51.750096°N, 7.993412°E), which is characterised by seven soil texture classes (Figure 1). A total of 60 soil profiles of 0.9 m depth were sampled at three soil layers (0 to 0.3 m, 0.3 to 0.6 m, 0.6 to 0.9 m), at six different dates (3 times in spring, 3 times in autumn) over a period of three years (2000 to 2002). Each sample was analysed for N_{min} and WC (ISO 14256, ISO 11461). Grid points on nested grids (Figure 1) were additionally sampled to a depth of 3 m in order to investigate the vertical distribution of soil mineral N (results not shown). Detailed information about the site and data were provided by Wallor et al. (2018). Soil samples used for the comparison of conventionally and sensory examined soil NO_3^- originate from two experimental fields: i) a long-term field experiment (LTFE) at Muencheberg, Germany (52.503748°N, 14.140469°E) and ii) a N fertilisation trial at Marquardt, Germany (52.457757°N, 12.966905°E). At Muencheberg, mixed samples were collected from the upper soil layer of 48 plots reflecting six fertilisation levels, each with eight repetitions. Sampling date was in October 2016 after harvest. The field trial at Marquardt consists of altogether 16 plots resulting from four fertilisation levels and four repetitions.

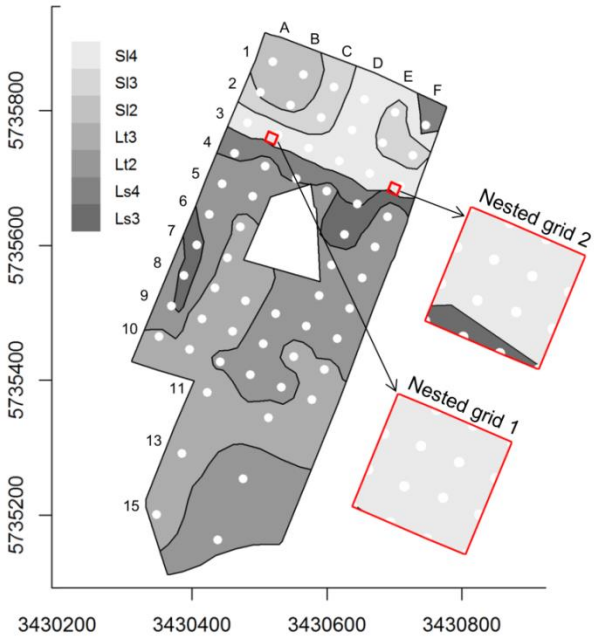

Figure 1. Beckum study site with location of grid points (regular grid: A1 to F10), nested grids and distribution of soil texture classes according to the German Soil Taxonomy (Ad-hoc AG Boden, 2005), aggregated over 0 to 0.9 m soil depth; clay content increases from Sl2 (5-8%) over Ls3 (17-25%) to Lt3 (35-45%).

At Marquardt, soil samples were collected from three soil layers (0 to 0.3 m, 0.3 to 0.6 m, 0.6 to 0.9 m) in February 2018. At both experimental fields soil texture is dominated by sand (67 to 90%).

Sampling strategies

The present study compares different soil sampling strategies with respect to the spatial and temporal variability of soil N available to plants using the Beckum data introduced above. The sampling strategies considered are according to Schirrmann et al. (2011) i) grid-based sampling practice in precision agriculture with one sampling point per hectare, ii) sampling practice based on soil inventory (zone-based) with one sampling point per soil unit and iii) intensive sampling (Table 1). The grid-based sampling practice was imitated by the randomised selection of 20 regular grid points from the entire pool. Regarding the zone-based sampling practice the regular grid points were assigned to the corresponding soil texture class and results of soil analysis were averaged accordingly (cf. Figure 1).

Table 1. Regular grid points considered in the analysis of each described sampling strategy.

Sampling strategies	Regular grid points included	Number of sample locations per ha (on average)
grid-based	A4, A5, A7, A9, B1, B3, C8, C9, C11, C13, C15, D1, D4, E3, E6, E8, E13, F1, F4, F10	n = 1.00 per ha
zone-based	points per soil texture class (cf. Figure 1)	n = 0.35 per ha*
intensive	all	n = 3.00 per ha

* referring to the mean value of all sampling points in one soil texture class

Sensor measurements

Ion selective electrodes (ISE) and a colorimetric sensor were tested with samples taken from Muencheberg and Marquardt. An ISE is a transducer that converts the concentration of a specific ion dissolved in a solution into an electrical potential. The ion-selective membrane is the key component of ISEs (Bomar et al., 2017). An ISE generates a difference in electrical potential between itself and a reference electrode. This potential is proportional to the concentration of the target ion (here: NO_3^-) in the solution (Rundle, 2011). Colorimetry is an optical method which uses reagents that change their colour in the presence of the analyte (Gautheyrou et al., 2001). The colour intensity, which is proportional to the concentration of the analyte, is measured by a photo diode at a defined wavelength. Soil samples were prepared according to Jones (2001) and afterwards the absorption factor was measured. The specific NO_3^- concentration was estimated using a pre-defined calibration equation and the Lambert-Beer Law (Mayerhöfer et al., 2016). The amount of absorbed light by the reacted sample is directly related to the amount of NO_3^- concentration. For comparing sensory and conventionally measured NO_3^- concentrations, results of the conventionally applied N_{min}-method (N_{min} = NO_3^--N+NH_4^+-N, ISO 14256) were multiplied by 44.268 (= 10 · 4.4268) to consider the difference in the dimensions (g $100g^{-1}$ → ppm) and to convert them into NO_3^- concentration (NO_3^--N → NO_3^-).

Tools and statistics

All statistical analyses have been conducted using the R software (Core Team R, 2018). The stratified sampling method from the *spsample* function in R (*gstat* package) (Bivand et al., 2013) was used to select grid points by geometry from the entire pool of the Beckum data to establish the grid-based sample (cf. Table 1). The *spsample* function marks a previously defined number of points in a field. In the case of the field examined here, the grid points closest to the *spsample* marks were selected. Results of soil mineral N as detected by the introduced sampling strategies where compared by using box and whisker plots (McGill et al., 1978). Differences between the distributions of measured soil states according to the soil texture zones were determined by the Mann-Whitney U-test (Mann and Whitney, 1947) due to deviations from the normal distribution of some data. For the comparison of the vertical distribution of soil mineral N within soil profiles averaged over all grid points and over grid points belonging to different soil texture classes, the package *SoilDB* was used (Beaudette et al., 2018). Conventionally and sensory measured NO_3^- contents in the soil samples were compared in a regression analysis. The quality of the corresponding regression models is described by Akaike's An Information Criterion (AIC) (Sakamoto et al., 1986).

Results

Sampling strategies & field-scale variability of soil states

When comparing the distributions of soil mineral N according to the introduced sampling strategies no significant differences could be detected with respect to its within-field variability. This applies to the vast number of sampling dates and soil depths considered in this study (Figure 2). Only the value range was considerably reduced by grouping and averaging measured soil states according to the soil inventory.

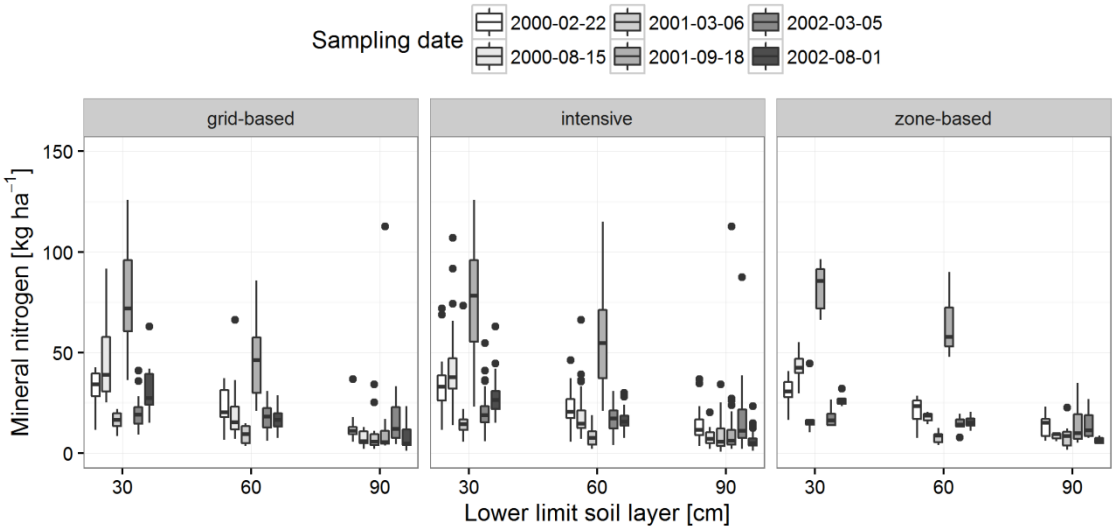

Figure 2. Field-scale variability of soil mineral N as detected by different sampling strategies at six sampling dates and for each soil layer; boxes refer to the lower and upper quartile (25th and 75th percentile), whiskers refer to the upper and lower extreme, and horizontals refer to the median.

In the grid-based sampling strategy the scattering of values declined due to a lower sample size. It also shows that some extremes are not captured by the grid-based sampling. As expected, the amount of soil mineral N is lower in spring than in autumn after harvest when looking at the same year. In addition, soil mineral N decreases with soil depth for each sampling date. In order to identify differences between the vertically aggregated soil texture classes N_{min} and WC results were divided by sampling dates (autumn, spring) and assigned to the corresponding soil texture class. Results are presented in Table 2. Obviously, differences between the units of the soil inventory are more pronounced for WC than for N_{min} (Figure 3) and, the zone-based variation of WC occurs more regularly over the year compared to N_{min}.

Table 2. Results of the Mann-Whitney U-test (Mann and Whitney, 1947); soil mineral N and WC values were grouped by spring and autumn sampling dates, soil layer and soil texture class; groups sharing the same letter do not show significant differences in the distribution of soil mineral N and WC, respectively.

Season	Soil state	Layer [m]	Soil texture class					
			Sl3	Sl4	Ls3	Ls4	Lt2	Lt3
Spring	Nmin	0-0.3	a	abc	b	abc	c	c
		0.3-0.6	a	abc	b	bc	c	c
		0.6-0.9	abc	ab	c	ac	b	abc
	WC	0-0.3	a	bc	b	c	d	d
		0.3-0.6	a	bc	b	c	d	d
		0.6-0.9	a	b	c	d	d	d
Autumn	Nmin	0-0.3	a	a	a	a	a	a
		0.3-0.6	a	a	a	a	a	a
		0.6-0.9	a	b	abcd	abc	d	c
	WC	0-0.3	a	b	b	b	c	d
		0.3-0.6	a	b	c	bc	d	e
		0.6-0.9	a	b	b	bc	c	c

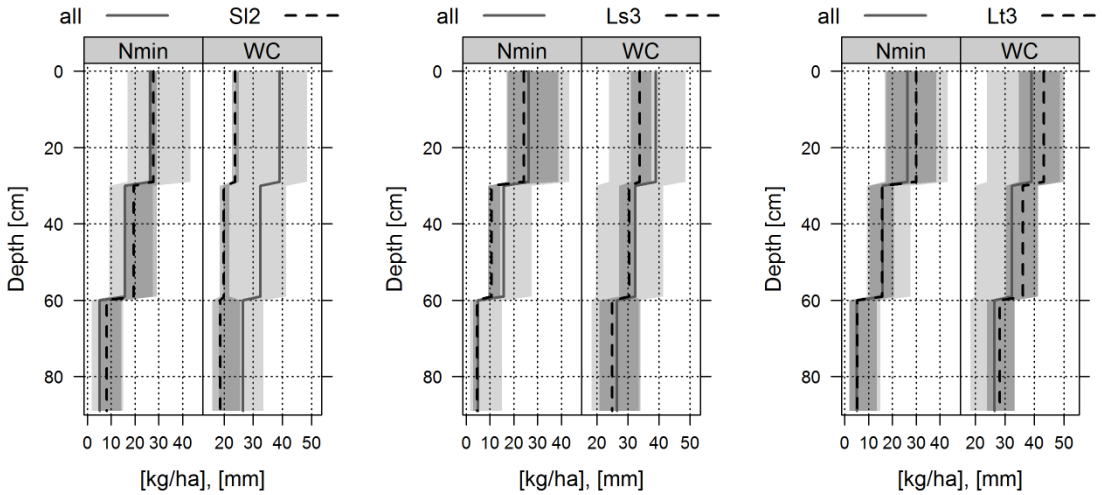

Figure 3. Comparison of soil mineral N and WC in the soil profile averaged over all regular grid points (grey) and over grid points belonging to different soil texture classes (black; Sl2, Ls3, and Lt3); sampling date 01.08.2002; plots show the median bounded by 5th and 95th percentiles.

The nitrogen state differs mainly in spring between soil texture classes. In autumn, variation in soil mineral N is present only in the soil layer of 0.6 to 0.9 m. However, compared to the overall sample the zone-based vertical distribution of mineral N shows slight differences, which is exemplarily shown for one sampling date in autumn (Figure 3). Furthermore, the range of measured N_{min} is the lowest in the upper layer of the sandy texture class Sl2.

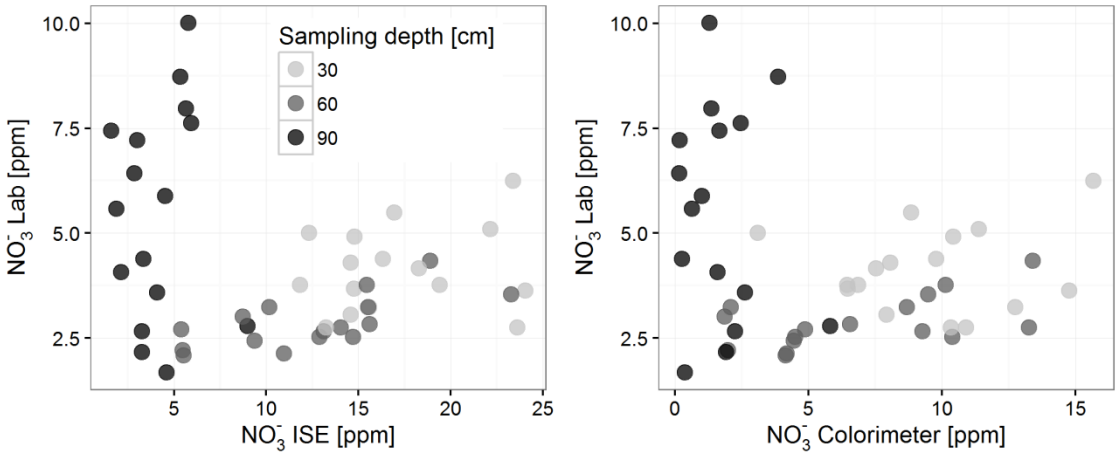

Figure 4. Relation between NO_3^- [ppm] measured conventionally in the laboratory and sensory by ISE and colorimeter; different point colours refer to individual sampling depths.

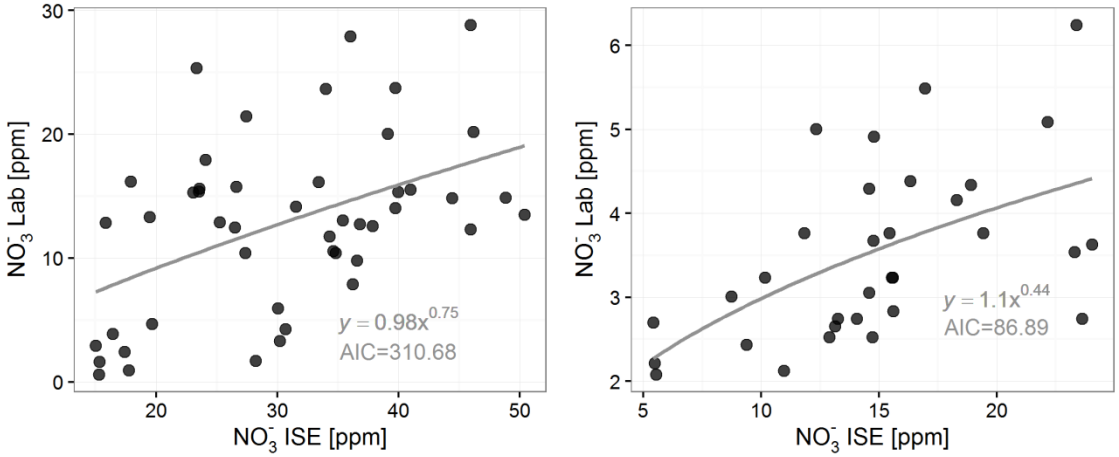

Figure 5. Relation between NO_3^- [ppm] measured conventionally in the laboratory and by ISE; left plot: samples from LTFE Muencheberg, samples were dried and sieved before ISE measurements; right plot: samples from the field trial at Marquardt, samples were measured field-fresh.

Sensory detection soil NO_3^-

The quality and type of relation between sensory and conventionally measured soil NO_3^- differs according to sampling depth and preparation of the sample. Figure 4 presents the results of NO_3^- measurements from the soil sampling at Marquardt, where three soil layers were considered and samples were analysed field-fresh. It becomes

obvious that samples from the lowest soil layer show no relation at all between sensory and conventionally measured soil NO_3^-. This is true for both sensors the ISE and the colorimeter. In total, ISE identifies higher NO_3^- contents than the colorimeter. In Figure 5 results from the comparative measurements of the Muencheberg and Marquardt sampling are depicted exclusively for the upper soil layer. In contrast to the Marquardt samples, the Muencheberg samples were dried and sieved before the sensory detection. Again, ISE values exceed the conventionally measured ones. Although, the AIC of the corresponding regression models is not comparable due to different samples' origin and range of NO_3^- values, results suggest an improved relation when samples are field-fresh. In that case, the regression is rather non-linear compared to the regression of prepared samples.

Discussion

Due to the highly mutable character of soil NO_3^- it has to be stated that a certain number of impact factors is not covered by the present study (pH-value, N_{total}, C_{total}, microbiology). However, it is common practice to determine the required nitrogen fertilisation rate on the base of one soil sampling autumn and/or spring before crop growth is accelerating. The extent of within-field variability is covered especially by the intensive and grid-based sampling strategy. Calculating the average soil mineral N based on all available grid points per each soil unit in the zone-based strategy causes a decline in the spans of the values for each sampling date. But from a practical point of view, the zone-based sampling strategy allows for the identification of quasi-homogeneous units in the field. Soil-related variations of mineral N were detectable especially for the spring sampling. However, the large observed within-field variability of soil mineral N underpins the need for its efficient detection in the field. Preliminary results of sensory measurements suggest an influence of soil organic carbon (SOC) on the detectability of NO_3^- by ISE and colorimeter. Referring to Figure 4 and the Marquardt sample the correlation between sensory and conventionally examined NO_3^- decreased considerably below 0.6 m sampling depth. In the corresponding soil layer SOC is the lowest and amounts to 0.18% per mass compared to 0.36% per mass and 0.77% per mass in the second and upper layer, respectively. Since the measuring principles of the two sensors used are quite different, there is also the possibility of a systematic error here. The correlation coefficient of the ISE and colorimeter outputs is 0.74 considering all Marquardt samples. The influence of sample preparation on the quality and type of regression and the generally higher levels of sensory detected soil NO_3^- need to be investigated more closely.

Conclusion

The comparison of sampling strategies has shown that intensive sampling produces the widest range of values as well as most outliers. This can lead to misinterpretations in the derivation of management zones. The texture-based sampling strategy is preferable to this, as there are clear differences between the soil types, especially during spring sampling, which is crucial for the planning of site-specific fertilization. The further development of reliable correlation functions for recording soil nitrate from sensor readings requires further reference analyses on different soil types from different soil depths.

References

Beaudette, D.E., Skovlin, J. and Roecker, S.M. (2018). soilDB: Soil Database Interface. R package version 2.0-1. http://CRAN.R-project.org/package=soilDB.

Bivand, R.S., Pebesma, E. and Gomez-Rubio, V. (2013). Applied spatial data analysis with R, Second edition. Springer, NY. http://www.asdar-book.org/

Bomar, E.M., Owens, G.S. and Murray, G.M. (2017). Nitrate Ion Selective Electrode Based on Ion Imprinted Poly(*N*-methylpyrrole). Chemosensors, 5(2), 1-8.

Core Team R, 2018. R: a Language and Environment for Statistical Computing. R Foundation for Statistical Computing, Austria, Vienna. Accessed 03 July 2018. http://www.R-project.org/.

Galloway, J.N., Aber, J.D., Erisman, J.W., Seitzinger, S.P., Howarth, R.W., Cowling, E.B. et al. (2003). The nitrogen cascade. BioScience 53(4), 341-356.

Gautheyrou, J., Loyer, J.Y. and Pansu, M. (2001). Soil Analysis. A.A. Balkema Publishers, India, ISBN 90-5410-716-2.

Gebbers, R., Dworak, V., Mahns, B., Weltzien, C., Büchele, D., Gornushkin, I., et al. (2016). Integrated approach to site-specific soil fertility management. In Proceedings of the 13th international conference on precision agriculture. Accessed 26 February 2019. www.ispag .org/proce eding s/?actio n=abstr act&id=2084&search=autho rs.

Giles, M., Morley, N., Baggs, E.M. and Daniell, T.J. (2012). Soil nitrate reducing processes - drivers, mechanisms for spatial variation, and significance for nitrous oxide production. Frontiers in Microbiology, 3(407), 1-16.

Jones, J.B. (2001). Laboratory Guide for Conducting Soil Tests and Plant Analysis. CRC Press, ISBN 9780849302060.

Mann, H. and Whitney, D. (1947). On a test of whether one of two random variables is stochastically larger than the other. Annals of Mathematical Statistics 18, 50–60.

Mayerhöfer, T.G., Mutschke, H. and Popp, J. (2016). Employing Theories Far beyond Their Limits—The Case of the (Boguer-) Beer–Lambert Law. ChemPhysChem 17(13), 1948–1955 doi:10.1002/cphc.201600114.

McGill, R., Tukey, J.W. and Larsen, W.A. (1978). Variations of box plots. The American Statistician 32, 12–16.

Nanni, M. R., Pinheiro Povh, F., Melo Demattê, J. A., de Oliveira, R. B., Chicati, M. L. and Cezar, E. (2011). Optimum size in grid soil sampling for variable rate application in site-specific management. Scientia Agricola, 68(3), 386–392.

Rundle, C.C. (2011). A Beginners Guide to Ion-Selective Electrode Measurements. Nico2000 Ltd, London. Accessed 26 February 2019 http://www.nico2000.net/Book/Guide1.html

Sakamoto, Y., Ishiguro, M. and Kitagawa G. (1986). Akaike Information Criterion Statistics. D. Reidel Publishing Company.

Schirrmann, M., Gebbers, R., Kramer, E., Seidel, J. (2011). Soil pH Mapping with an On-The-Go Sensor. Sensors 11, 573-598.

Wallor, E., Kersebaum, K.C., Lorenz, K. and Gebbers, R. (2018). A comprehensive dataset demonstrating the within-field variability of soil properties and crop growth conditions in northwestern Germany. Open Data Journal for Agricultural Research, vol. 5, 1-10.